On Drag of Circular Cylinder Suspended in uniform viscous Flow

-Application to Tension Thread Flow Meter-

Ai Nakagawa and Takeo, R.M. Nakagawa

Academy of Hakusan, 2-14, Meiko, Hakusan 920-2152 Japan

takeonakagawa8@gmail.com

Abstract

This paper is concerned with an exact solution of a circular cylinder in uniform viscous flow and its application to a flowmeter named Tension Thread Flow Meter. An analytical procedure to lead the exact solution for a drag of a circular cylinder suspended in a uniform viscous flow has been demonstrated, and it is found that the drag is proportional to the square of velocity weakly rather than the linear dependency on the velocity, as Stokes law for a sphere. When the Reynolds number Re < 0.4, the relation between the drag coefficient Cf and Re, as well as the drag of a circular cylinder in uniform flow and Re, have been derived and presented as simple analytical expressions. The theoretical results on the drag of a circular cylinder in a uniform flow have been applied directly to the prototype flowmeter, and to the velocity calibration for the selected scales of the thread, and their arrangements together with the velocity range, to be used. A prototype flowmeter has been manufactured and then deployed successfully to measure three velocity components in oscillatory waves. It is suggested that the potential of the flowmeter is almost limitless so that it is strongly recommended to develop the commercial version for general users, who are interested in measuring boundary layer flow, oscillatory wave, and turbulence.

Keywords: Drag, Cylinder, Viscous Flow, Flowmeter, Oscillatory Flow, Turbulence

1. Introduction

Navier-Stokes equations have been accepted as the basic equation describing motion of flows for nearly two centuries (Navier 1827, Stokes 1845). However, this view was objected by Tsugé(1969), because Navier-Stokes equation is only valid when the flow is laminar, but not for turbulent flow. At latest, until 1969, Tsugé had gotten a belief that Navier-Stokes equations are not applicable for turbulent flow, so that he started to formulate alternative equation to solve turbulent problems on the basis of kinetic theory, for he considered that unless one views motion of flow microscopically, it is impossible to know the true behavior of fluid motion. Refer to Nakagawa (2006) for more details on Tsugé's work on turbulence. This is the main reason why the present authors have neither interest in solving turbulent flow by using Navier-Stokes equation, nor results obtained by the equation.

In the meanwhile, the present authors are required to have the detail knowledge concerning to the drag exerted on a circular cylinder suspended in a uniform flow at low Reynolds number in order to develop a novel flow meter, called Tension Thread Flow Meter(referred to TTFM hereafter). Thus, an extensive literature survey on the relevant papers (e.g. Wieselsberger 1921, Richards 1934) has been conducted, and it is found that Lamb (1932) reported useful formula on the drag of two-dimensional elliptic cylinder moving in a fluid with constant velocity U in the form

$D_{elliptic}=4\pi\mu U/〚a/(a+b)-\gamma-\ln[U/(8\nu)\cdot(a+b)〛$, (1)

where π is ratio of circumference, μ the dynamic viscosity, a the semi-axis being parallel to the flow, b the other semi-axis normal to the flow, $\gamma=\lim_{n=\infty}(1+1/2+1/3+\cdots+1/n-\ln\cdot n)=0.57721$ Euler constant, and ν the kinematic viscosity. In (1), when a=0, we have the drag of a plate placed normal to the flow direction, while when b=0, it gives the drag of a plate parallel to the flow direction.

In this study, a review on the formula for the drag of a circular cylinder has been made with reference to the design of TTFM, because this knowledge is essential for the further development or improvement.

2. Theoretical

The Navier-Stokes equations with no external forces may be expressed by

$\nu\nabla^2u=(1/\rho)\partial p/\partial x+\partial u/\partial t+u\partial u/\partial x+v\partial u/\partial y+w\partial u/\partial z,$

$\nu\nabla^2v=(1/\rho)\partial p/\partial y+\partial v/\partial t+u\partial v/\partial x+v\partial v/\partial y+w\partial v/\partial z,$ (2)

$\nu\nabla^2w=(1/\rho)\partial p/\partial z+\partial w/\partial t+u\partial w/\partial x+v\partial w/\partial y+w\partial w/\partial z,$ and

the equation of continuity is

$\partial\rho/\partial t+\partial(\rho u)/\partial x+\partial(\rho v)/\partial y+\partial(\rho w)/\partial z=0.$ (3)

By neglecting the inertia terms in Navier-Stokes equations, we have equations of motion in a viscous liquid. When external forces are absent, if we attempt to find the steady and incompressible fluid (ρ=const.), motion produced by the translation of circular cylinder with constant velocity U through an infinite mass of liquid, (2) and (3) become simplified equations, respectively.

$\mu\nabla^2u=\partial p/\partial x,$

$\mu\nabla^2v=\partial p/\partial y,$ (4)

$\mu\nabla^2w=\partial p/\partial z,$

and

$\partial u/\partial x+\partial v/\partial y+\partial w/\partial z=0.$ (5)

However, (4) and (5) prove to be impossible to satisfy all of the required conditions. This was pointed out by Stokes, who gave the following remark: "The pressure of the cylinder on the fluid continually tends to increase the quantity of fluid with which it carries, while the friction of the fluid at a distance from the cylinder continually tends to diminish it. In the case of a sphere, these two cause eventually counteract each other, and so the motion becomes uniform. But in the case of a cylinder, the increase in the quantity of fluid carried continually gains on the decrease due to the friction of the surrounding fluid, and the quantity carried increases indefinitely as the cylinder moves on".

It appears, however, that if the inertia-terms in (2) are partially taken into account, the Stokes remark may be modified, and a definite value of the drag on the circular cylinder is obtained as follows:

Equation (2) are satisfied by

$u=-\partial\phi/\partial x+[1/(2k)]\cdot\partial\chi/\partial x-\chi$,

$v=-\partial\phi/\partial y+[1/(2k)]\cdot\partial\chi/\partial y$, (6)

where ϕ is velocity potential, and

$p=\rho U\partial\phi/\partial x$, (7)

provided

$\nabla_1^2\phi=0$, (8)

and

$(\nabla_1^2-2k\cdot\partial/\partial x)\chi=0$. (9)

The solution of (9) is

$\chi=c\cdot e^{kx}\int_0^\infty e^{-krcosh\omega}d\omega$. (10)

For the definite integral, we have the expansions,

$\int_0^\infty e^{-krcosh\omega}d\omega=[\pi/(2kr)]e^{-kr}\ [\![1-1^2/(8kr)+1^2\cdot3^2/[1\cdot2(8kr)]-...]\!]$, (11)

which is suitable for large values of kr. On one hand, for small values of kr, we get

$\chi=-c(1+kr)[\gamma+ln(1/2)\cdot(kr)]$, (12)

with

$(1/(2k)\cdot\partial\chi/\partial x-\chi=-[c/(2k)]\cdot[k(1/2-\gamma-lnkr/2)+\partial lnr/\partial x-kr^2/2\cdot\partial^2lnr/\partial x^2+...]$,

$(1/(2k)\cdot\partial\chi/\partial y=-[c/(2k)]\cdot(\partial lnr/\partial y-kr^2/2\cdot\partial^2lnr/\partial x\partial y+...)$. (13)

Hence, if we put the velocity potential,

$\phi=A_0lnr+A_1\partial lnr/\partial x+...$, (14)

we find that the condition $u=-U$, $v=0$, and $w=0$ will be satisfied for $r=a$, provided

$c=2U/[1/2-\gamma-ln(ka/2)]$, $A_0=-c/(2k)$, $A_1=ca^2/4$, (15)

approximately. Thus, near the cylinder, we obtain

$u=(1/2)\cdot c[\gamma-\frac{1}{2}+ln(kr/2)+(r^2-a^2)/2\cdot\partial^2lnr/\partial x^2]$,

$v=c/4\cdot(r^2-a^2)\cdot\partial^2lnr/\partial x\partial y$. (16)

The vorticity is given by

$\zeta=\partial v/\partial x-\partial u/\partial y=c\cdot e^{kz}\cdot\partial(\int_0^\infty e^{-krcosh\omega}\cdot d\omega$,

which for large values of kr takes the form,

$\zeta=-kc\cdot(y/r)[\pi/(2kr)]^{1/2}e^{-k(r-x)}$. (17)

To calculate the force exerted by the fluid on the cylinder, we have to integrate the expression,

$r \cdot p_{rx} = -px + \frac{\mu r \partial u}{\partial r} + \mu(x\partial u/\partial x + y\partial v/\partial x)$. (18)

with respect to the angular coordinate θ from 0 to 2π. The first term of (18) gives, when r is put equal to a,

$-\rho U A_0 \int_0^{2\pi} cos^2\theta d\theta = -\pi\rho U A_0 = \pi\mu\theta$. (19)

The second term contributes, on substitution from (16), πμc. The third term gives a zero result, to our order of approximation. The final value for the drag $D_{cylinder}$ per unit length of a circular cylinder is, therefore, expressed as,

$D_{cylinder} = 2\pi\mu c - 4\pi\mu U/[1/2 - \gamma - \ln(1/4 \cdot Ua/\nu)$, (20)

when the Reynolds number $Re = Ua/\nu$ is smaller than 1, where π is the ratio of circumference, μ the dynamic viscosity of the fluid, U the flow velocity, γ the Euler constant, a the radius of cylinder, and ν the kinematic viscosity of fluid. Equation (20)

may be written as,

$D_{cylinder} = 4\pi\mu U/[1/2 - \gamma - \ln(Re/4)]$, (21)

On one hand, introducing the conventional expression of drag, we put formally,

$D_{cylinde} = 1/2 \cdot C_f \rho U^2 S$, (22),

where C_f is drag coefficient, ρ the fluid density, S the projected area of the circular cylinder on the plane normal to the flow direction. Since S=a for the unit length of the cylinder, (21) and (22) gives us the drag coefficient as,

$C_f = 8\pi Re^{-1}/(\ln Re^{-1} - \epsilon)$, (23)

with

$\epsilon = 0.077$.

This formula is valuable in practical point of view: (21) is an exact solution of Navier-Stokes equation, and thus it is considered to be valid if the Reynolds number is smaller than 1. That is, we can obtain the drag by inserting the value of Re, and the velocity U into (21) easily.

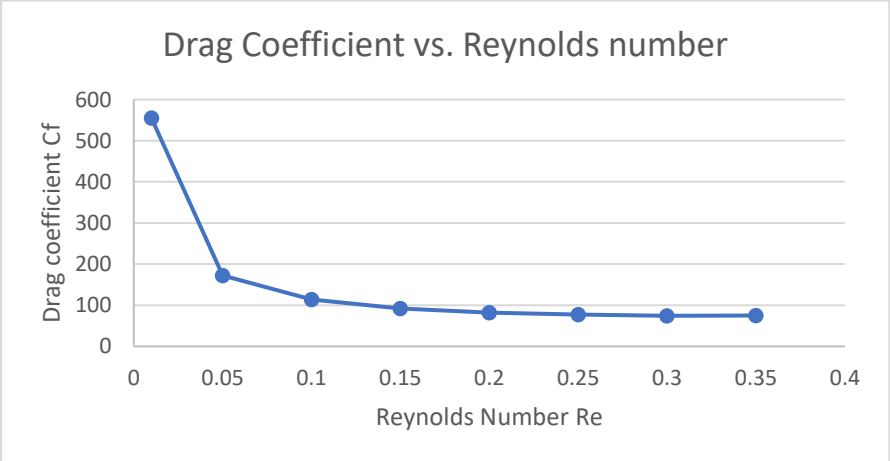

Fig. 1 Drag coefficient against Reynolds number.

Fig.1 shows the relation of the drag coefficient C_f against the Reynolds number Re.

It can be seen that C_f decreases with increasing Re gradually, and takes almost constant value of 75 once Re exceeds to the value of 0.2.

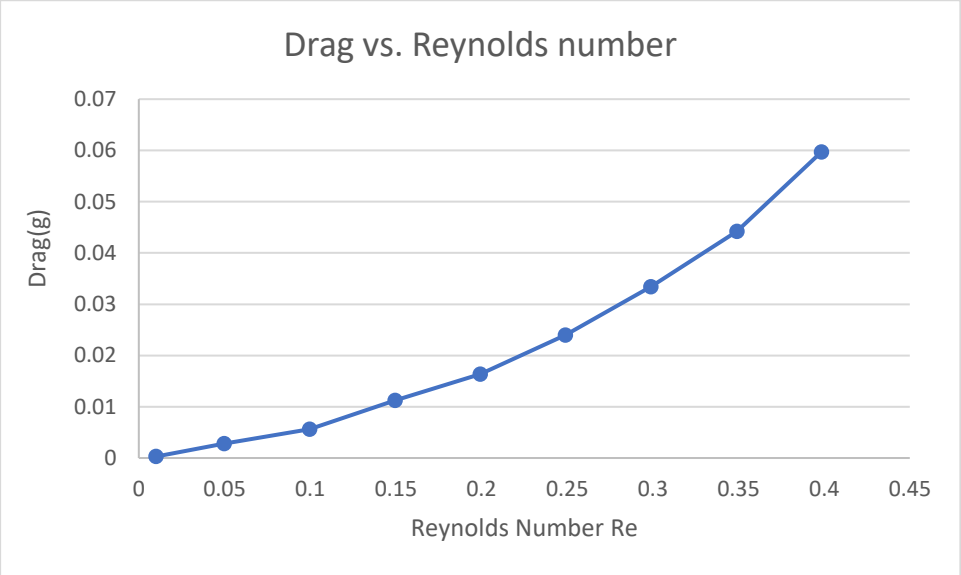

Fig. 2 Drag against Reynolds number.

Fig.2 denotes that the drag $D_{cylinder}$ increases with the Reynolds number Re along the quadratic curve in this range of the Reynolds number $Re=Ua/\nu$. In another words, The drag depends on the square of the velocity U^2 weakly.

It may be worth comparing with the drag $D_{cylinder}$ with the drag D_{sphere} in the uniform velocity. The latter was derived by Stokes (1851) theoretically as

$D_{sphere}=6\pi\mu rU$

or

$D_{sphere}=C_f(Re)\cdot(1/2)\cdot \rho U^2 S$,

with

$C_f=24/Re$, $Re=Ur/\nu$, and $S=\pi r^2$,

where μ is the dynamic viscosity, and r the radius of the sphere, U the velocity, C_f the drag coefficient, Re the Reynolds number, ρ.the fluid density, and S the projected area of the sphere. In case of the sphere, the drag D_{sphere} depends on the Reynold number linearly in this range of the Reynolds number, viz. $Re < 1.0$.

3. Experimental

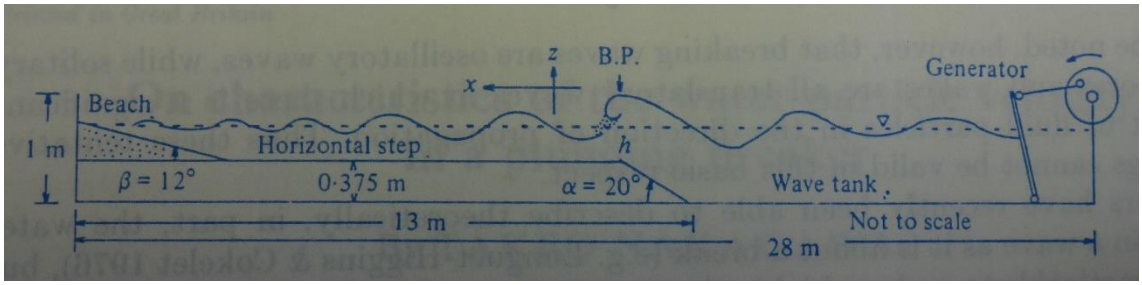

Fig.3 Schematic diagram of the experimental set-up.

Fig.3 shows a schematic diagram of the experimental set-up (Nakagawa 1983). The two-dimensional wave tank is 0.7m wide. The wave generator is a hybrid type of piston and flap.

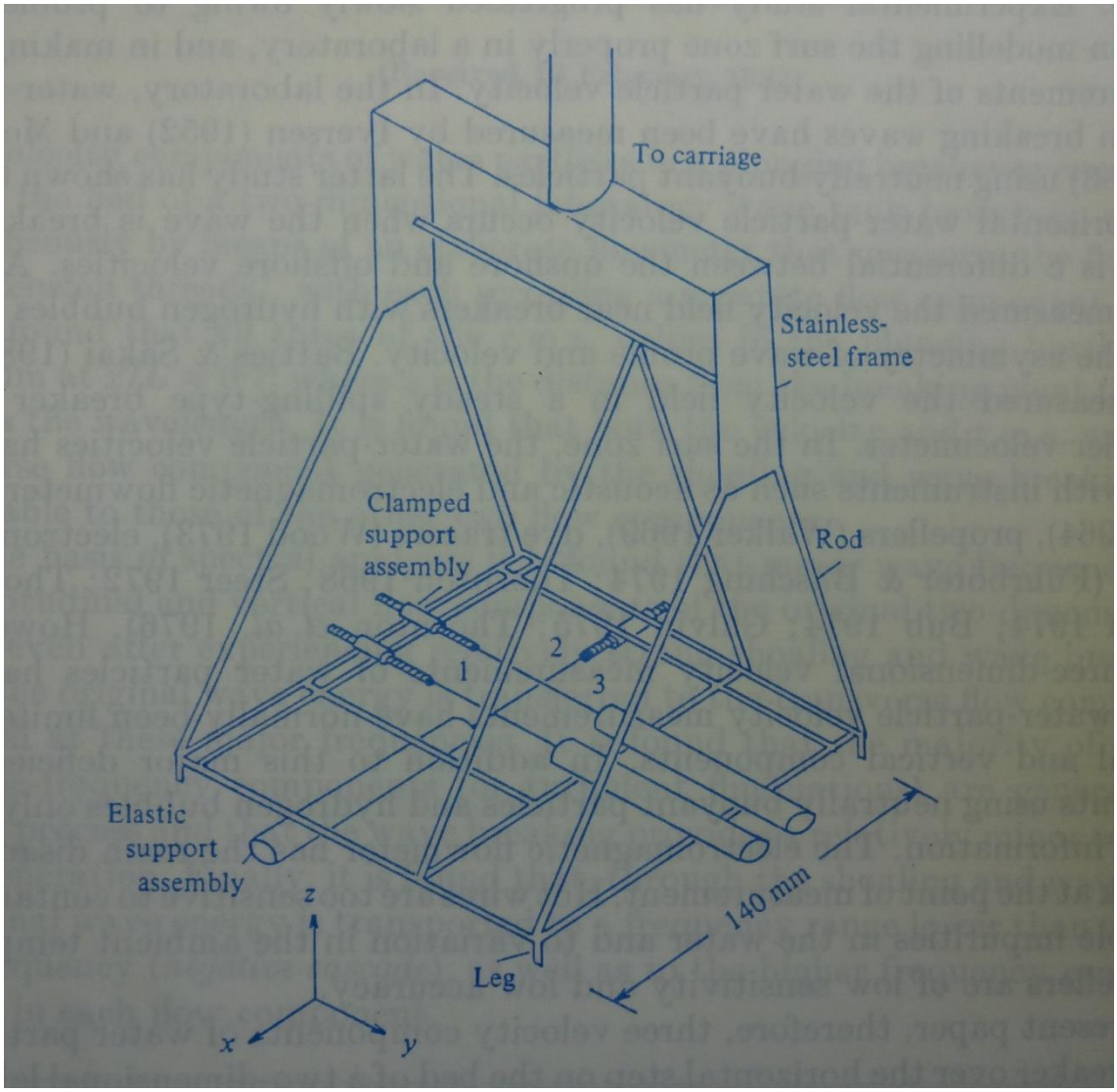

Fig.4 General view of the Tension Thread Flow Meter.

Fig.4 shows a general view of TTFM. The flow velocity is measured by the three cotton threads [1], [2] and [3], which measure velocities in the x-, y- and z-directions, respectively.

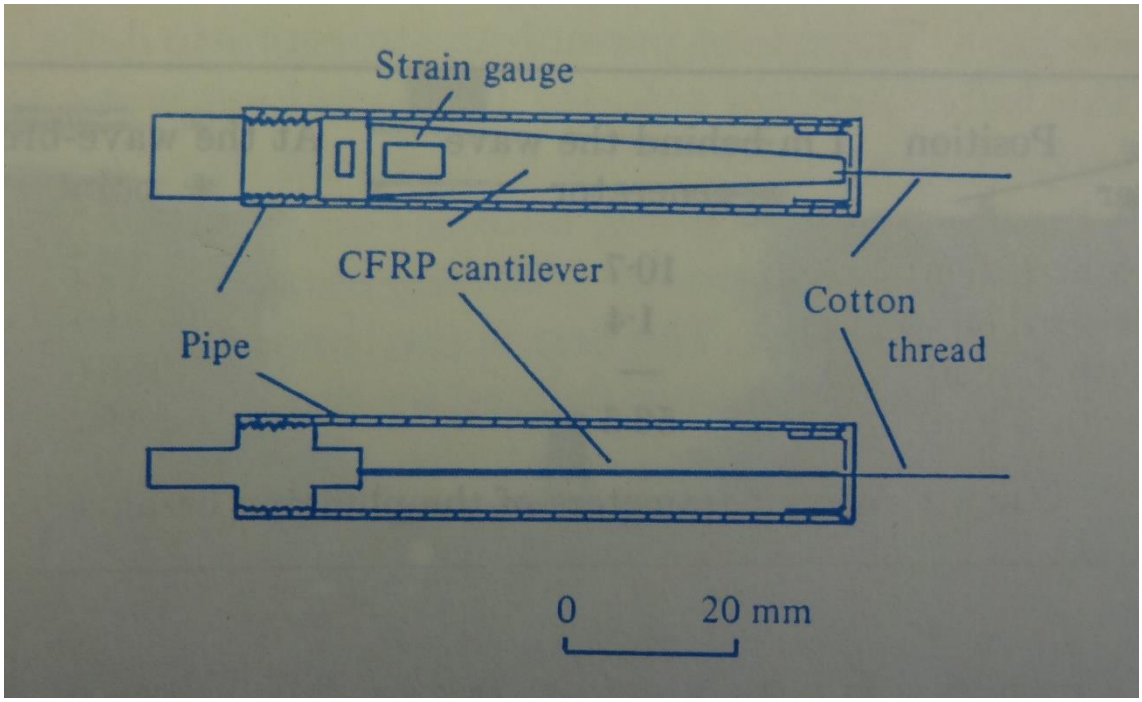

Fig.5 Cross-sections of the elastic support assembly.

The cross-sections of the elastic support assembly through the pipe axis are shown in Fig.5. The upper cross-section includes the plane of the cantilever of thickness 0.5mm, whereas the lower cross-section is normal to the plane. One end of the thread is fixed rigidly to the head of the screw rod, while the other end is knotted at the free end of the cantilever, so that it is supported elastically. Initial tension in the thread is controllable within a certain limit by adjusting the horizontal position of the screw rod. A semiconductor strain gauge of 120 Ω is glued on each surface of the cantilever, which is made of CFRP (carbon-fiber-reinforced plastic) of specific weight 1.7 and Young modulus $1.96 \cdot 10^5$ N/mm^2. The length and the diameter of all the threads are 55mm and 0.01mm, respectively. Threads [1] and [3] are suspended in the same horizontal plane, and are parallel each other and separated by 20mm. Thread [2] is in a horizontal plane at 15mm below the plane including threads [1] and [3], but it is normal to them. It is, therefore, clear that the velocity measured by the flowmeter is an integrated mean velocity in the small space, where the three threads are suspended: In the data analysis, however, the geometrical center of the three midpoints of the threads is assumed as the measuring point.

An increase of the thread tension due to the flow produces a small deflection of the cantilever and thus a strain in the gauges. Each of the threads can measure a separate velocity component normal to the respective plane of the cantilever, because the ratio of the width to the thickness is sufficiently large: The ratio is 6 and 16 at the tip and base of the cantilever, respectively. In general, the flow drag on a thread is not linearly proportional to the velocity, but is proportional to square of the velocity, as being elucidated theoretically in section 3, and shown in Fig.2.

Two strain gauges glued to the surface of a cantilever and a bridge box constitute an AC Wheatstone bridge, and the out-of-balance electrical signal is amplified by a dynamic amplifier and then recorded on magnetic tape.

Calibrations of the present flowmeter have been made in a tank filled with still water. The plane of the cantilever is carefully set normal to the longitudinal axis of the tank. The flowmeter is then towed along the axis at a specified speed in the water and the output electrical signal is recorded on the tape. In this way, the flowmeter has been calibrated in the velocity range 3.0 ~120cm/s.

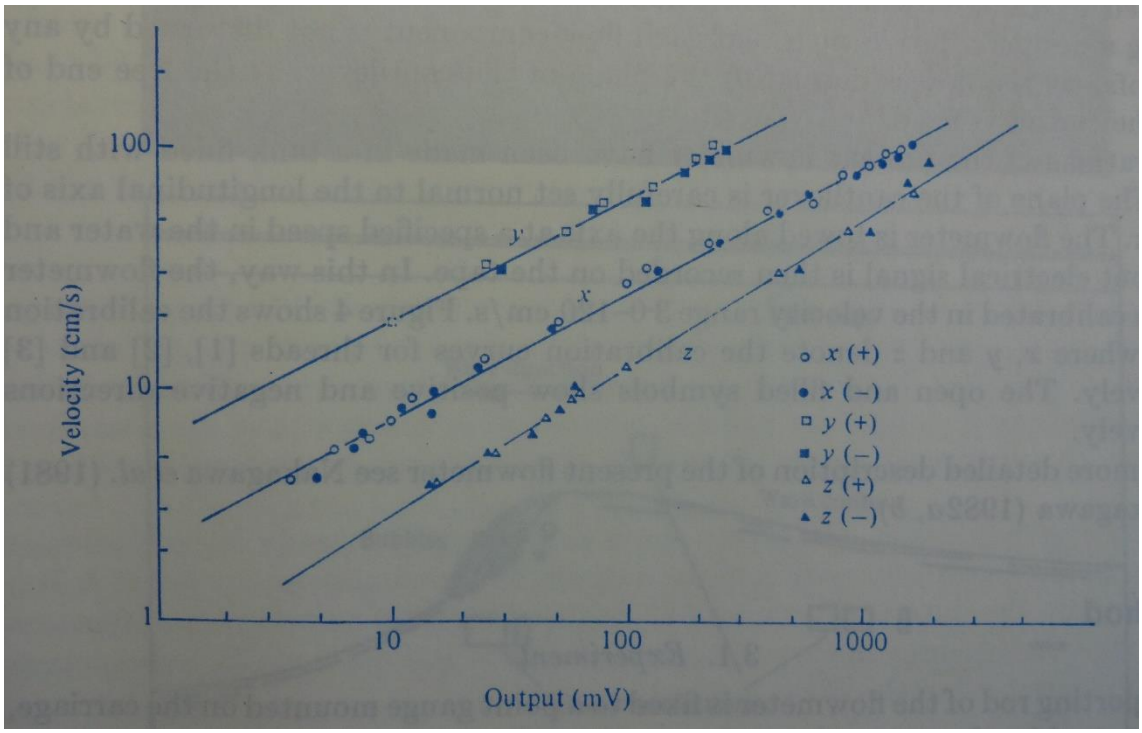

Fig. 6 Velocity calibration curves.

Fig.6 shows the calibration curves, where x, y and z denote the calibration curves for threads [1], [2] and [3], respectively.

4. Results and Discussion

The supporting rod of the flowmeter is fixed to a point gauge mounted on the carriage, which is capable of moving along the parallel rails on the upper edge of the wave tank (Fig.3). The vertical position of the flowmeter is thus adjusted by turning the point gauge knob. During measurements of the flow velocity, time histories of the water-surface elevation have been obtained with two capacitance-type wave-gauges concurrently. Water surface elevations are measured 1.0m behind the wave generator and at the same longitudinal position where TTFM is set to measure the flow velocity.

The flow velocities (u, v, w) are first separated into the steady flows (U,V,W) and the unsteady flows($\hat{u}$, $\hat{v}$, $\hat{w}$).

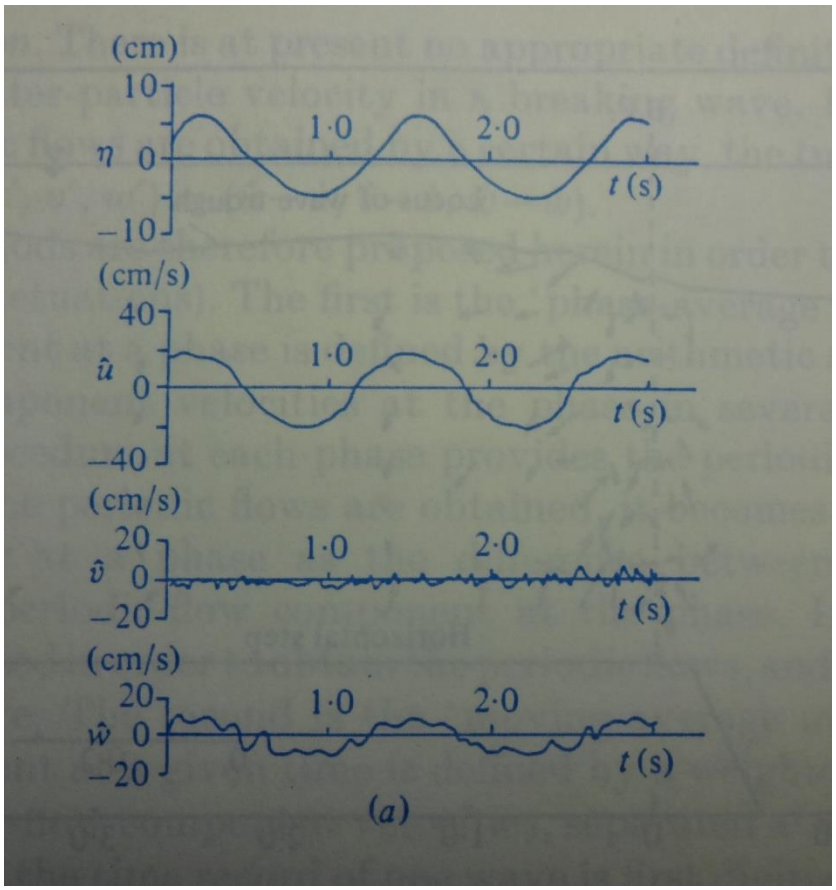
(cm)
10
η 0
−10
1·0
2·0
t (s)
(cm/s)
40
û 0
−40
1·0
2·0
t (s)
(cm/s)
20
v̂ 0
−20
1·0
2·0
t (s)
(cm/s)
20
ŵ 0
−20
1·0
2·0
t (s)
(a)

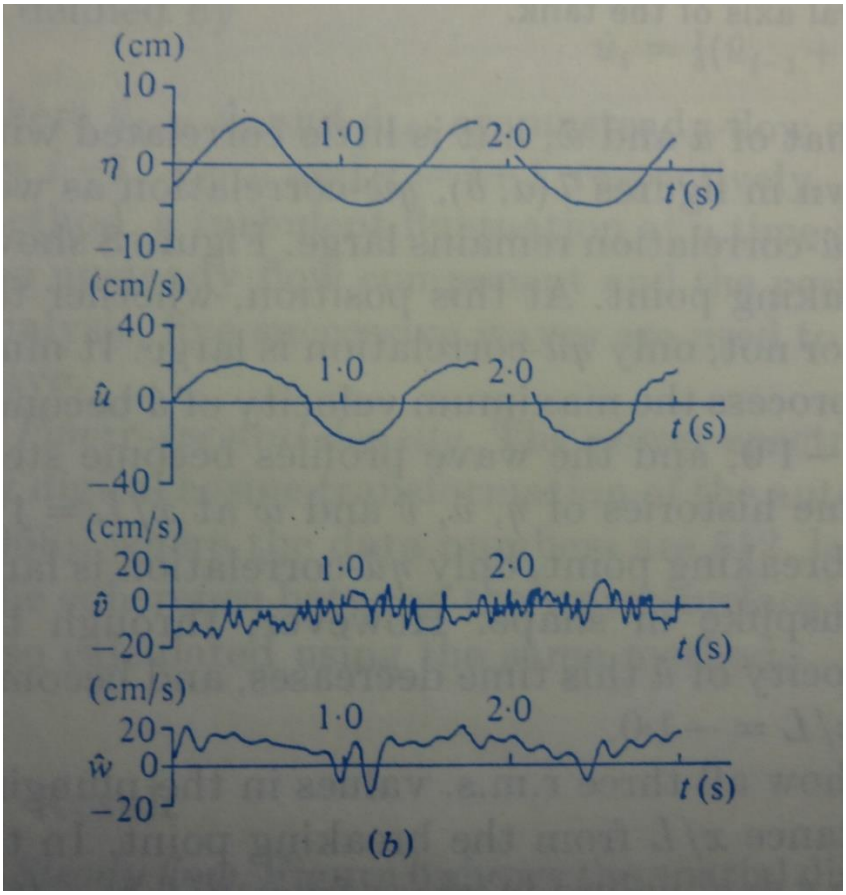
(cm)
10
η 0
−10
1·0
2·0
t (s)
(cm/s)
40
û 0
−40
1·0
2·0
t (s)
(cm/s)
20
v̂ 0
−20
1·0
2·0
t (s)
(cm/s)
20
ŵ 0
−20
1·0
2·0
t (s)
(b)

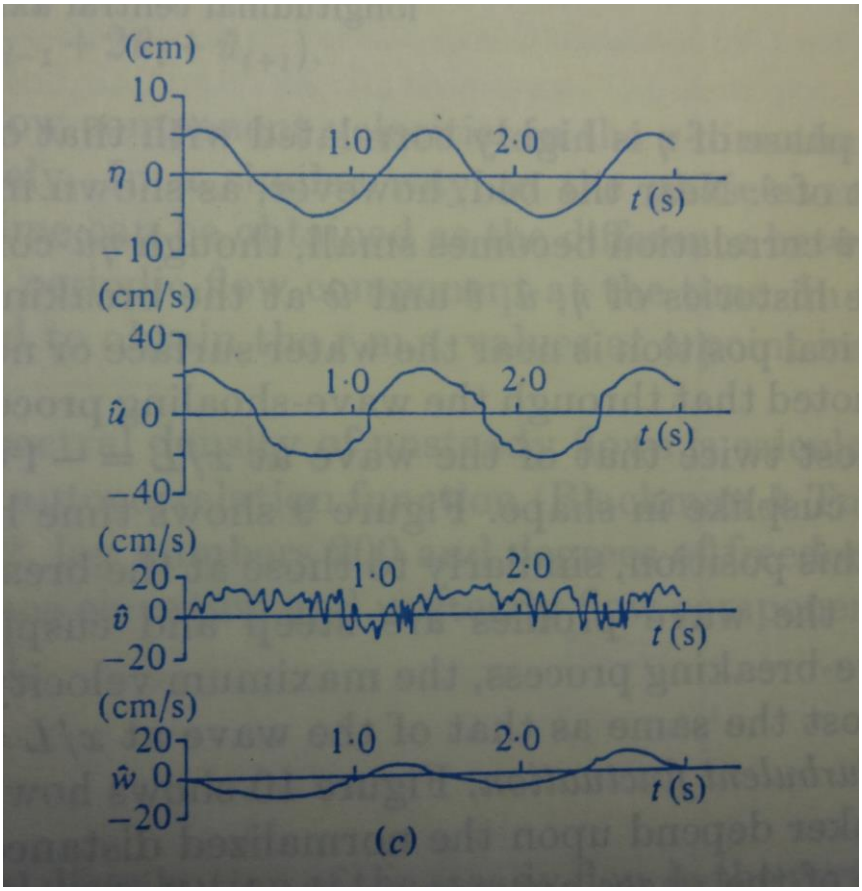

Fig.7 Time histories of η, $\hat{u}$, $\hat{v}$ and $\hat{w}$, before shoaling and wave breaking.

(a) 2 cm above the tank bed, (b) 8 cm above the tank bed, (c) 2 cm below the wave trough.

Fig.7 illustrates time histories of the water surface elevation η and the unsteady flows ($\hat{u}$, $\hat{v}$, $\hat{w}$) at x/L=−1.0, which is the longitudinal position on this side of wave breaking point by just one wavelength L. The wave at this position has not yet experienced neither shoaling nor breaking. It may be seen in this figure that the wave profiles are almost sinusoidal, with small deformations. Near the water surface, as shown in Fig.7(c), the phase of η is highly correlated with that of $\hat{u}$ and $\hat{w}$, but is little correlated with that of $\hat{v}$. Near the bed, however, as shown in Fig.7 (a,b), η$\hat{w}$-correlation as well as η$\hat{v}$-correlation becomes small, though η$\hat{u}$-correlation remains large.

5. Conclusions

In this section, new knowledge and insights obtained through the present study have been summarized:

1. An analytical procedure to lead the exact solution for drag of a circular cylinder suspended in a uniform viscous flow has been demonstrated, and it is found that the drag is proportional to the square of velocity weakly rather than the linear dependency on the velocity, as Stokes law for a sphere.
2. When the Reynolds number Re < 0.4, the relation between the drag coefficient C_f and Re, as well as the drag of a circular cylinder in a uniform flow and Re, have been derived and presented as simple analytical expressions.

3. The theoretical results on the drag of a circular cylinder in a uniform viscous flow have been applied directly to the prototype Tension Thread Flow Meter (TTFM), and the velocity calibration with respect to the selected scales of the thread, and their arrangements together with the velocity range, to be used.
4. A prototype TTFM have been manufactured and then deployed successfully to measure three velocity components in an oscillatory waves.
5. It is suggested that the potential of TTFM is almost limitless, so that it is strongly recommended to develop commercial version of TTFM for general users, who are interested in measuring boundary layer flow, oscillatory wave, and/or turbulence.

References

Lamb, H.(1932) Hydrodynamics. 6th Edition, Cambridge University Press, Cambridge. pp.738.

Nakagawa, T. (1983) On characteristics of the water-particle velocity in a plunging breaker. J. Fluid Mech. 126, 251-268. https://doi.org/10.1017/S0022112083000142

Nakagawa, T. (2006) Philosophy of Flow. vol.10, Scientific Papers on Turbulence by Shunichi Tsugé. Columbus University Press, Hakusan, pp.304.

Navier, M. (1827) Mémoire sur les Lois du Mouvment des Fluides. Mém. de l'Acad. d. Sci. 6, 389-416.

Richards, G.J.(1934) On the motion of an elliptic cylinder through a viscous fluid. Philosophical Transactions of the Royal Society of London, A233, 279-301. https://doi.org/10.1098/rsta.1934.0019

Stokes, G.G. (1845) On the theories of internal friction of fluids in motion. Trans. Cambr. Phil. Soc. B, 287-305.

Stokes, G.G. (1851) On the effect of the internal friction of fluids on the motion of pendulums. Transaction of Cambridge Philosophical Society, 9, 8-106.

Tsugé, S. (1969) A theory of fluctuation based on the hierarchy equation. Physics Letters 24A, 235-236. https://doi.org/10.1016/0375-9601(68)90621-X

Tsugé, S.(1974) Approach to the origin of turbulence on the basis of two-point kinetic theory. Phys. Fluids 17, 22-33. https://doi.org/10.1063/1.1694592

Wieselsberger, C. (1920) Der Luftwiderstand von Kugeln. AFM, 5, 140-144.